

A Multi-Scale Detection Technique for Anomaly on Ocean Surface Using Optical Satellite Images

Chi-Farn Chen and Li-Yu Chang

Center for Space and Remote Sensing Research, National Central University, Chinese Taipei

ABSTRACT

Using satellite images for monitoring oceanic surface has become popular recently. One of the striking feature can be detected from satellite image is the anomalous phenomenon on oceanic surface. In general, it is easy to observe the diversified anomalies, caused by abrupt change of the reflectance on oceanic surface, on the optical satellite images. Among them, the anomaly caused by the pollution of oil spill or discharge of waste water is commonly observed. In this study, a multi-scale detection technique for studying anomaly on oceanic surface from optical satellite image is proposed. The study uses a RX algorithm at first to measure the degree of anomaly for each image pixel. Next, a series of Laplace of Gaussian operators at different scale are applied to extract the possible anomalous patches in different size. Finally, a threshold from the cumulative distribution of the RX algorithm's output is used to extract final anomalous patches. Experiment results show that the proposed method can extract striking anomalous patches at offshore or open water areas in different optical satellite images.

Keywords: Anomaly, Multi-Scale Detection, Satellite Images

1. INTRODUCTION

The radiant intensity at optical sensor is directly related to the reflectance of target. For anomalous targets on ocean surface, their reflectance usually varies a lot with respect the background. Therefore, the anomalous phenomena on ocean surface can be easily distinguished in optical sensors. In general, the causes to form different kinds of anomalies are diverse. The most common example is the anomaly causes by the pollution of oil spill (Brown and Fingas, 2001) or discharge of waste water (Keeler *et al.*, 2005). Theoretically, it is not difficult to develop an algorithm to extract those kinds of anomalies from images acquired from optical sensors. In fact, the reflectance responses for ocean surface and its related phenomena generally tend to be very low. This effect makes anomalies on ocean surface be affected by noise very easily. Especially for those anomalies have reflectance much lower than normal sea water. Consequently, it is not possible to set a clear threshold to extract anomalies from background.

2. METHODOLOGY

In this study, a multi-scale detection technique for anomaly on ocean surface from optical satellite image is proposed. The method can be divided into three sections: (1) A RX algorithm (Reed and Yu,

1990) is used at beginning to measure the degree of anomaly for each image pixel from multi-spectral satellite image. (2) For reducing the effect of noise, a series of Laplace of Gaussian operators (Pratt, 1991) at different scale are applied to extract the possible anomalous patches in different size. (3) A threshold from the cumulative distribution of the RX algorithm's output is used to extract final anomalous patches.

2.1 Measuring the degree of anomaly using RX algorithm

The RX algorithm shown in equation (1) actually is no more than a method to retrieve the normalized spectral distance for each pixel from multi-spectral image with respect to image mean.

$$\delta_{RXD}(r) = (r - \mu)^T K_{L^*L}^{-1} (r - \mu) \quad (1)$$

where

K : Covariance matrix of source image.

r : Spectral vector of each pixel.

μ : Image mean.

Originally, RX algorithm is also a method used to extract anomaly from remotely sensed images (Chang and Heinz, 2000). However, the most important assumption for using this algorithm is that the amount of anomalies should much less than the background. In fact, this assumption may

not be hold because we actually do not know how much less is the anomalies. In addition, a clear threshold has to be set in this algorithm. This is also not practical for the noisy nature of out data.

2.2 Filtering possible anomalous patches using Laplace of Gaussian operation

Generally speaking, the anomalies are the areas that greater than mean value in normalized distance image. On the other hand, the convex areas of normalized distance image may be potential areas of anomalies. For the purpose to detect convex areas, a second order derivative operator “Laplace of Gaussian” is introduced.

In fact, Laplace of Gaussian is the Laplace of a Gaussian smooth operator. Equation (2) is a 2 dimensional Gaussian smooth operator with standard deviation “s”. Equation (3) is the Laplace of Gaussian operator. Fig. 1 illustrates the pattern of Laplace of Gaussian operator.

$$G(x, y) = \frac{1}{\sqrt{2\pi s^2}} \exp\left(-\frac{x^2 + y^2}{2s^2}\right) \quad (2)$$

$$\nabla^2 G(x, y) = \frac{1}{\pi s^4} \left[1 - \frac{x^2 + y^2}{2s^2} \right] \cdot e^{-\frac{x^2 + y^2}{2s^2}} \quad (3)$$

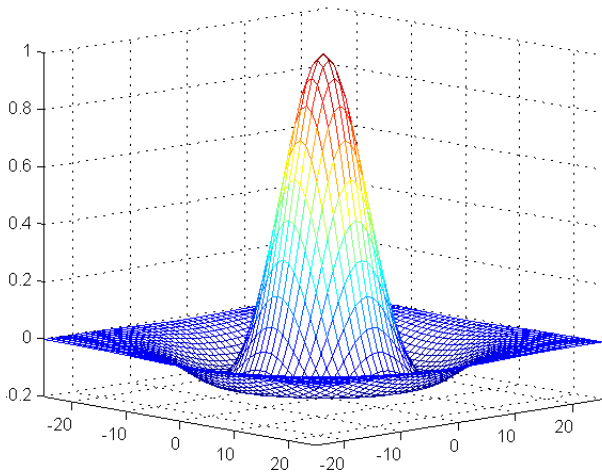


Fig. 1: The pattern of Laplace of Gaussian operator

Different scale of Laplace of Gaussian operator can be acquired by adjusting “s” parameters. The larger of “s” is used, the more smooth effect is achieved. Therefore, convex areas in different scales can be acquired by following procedure:

2.2.1.1 Convolving the normalized distance image with different scale of Laplace of Gaussian operator.

2.2.1.2 Taking positive part of the convolution output.

The following step in this section is to integrate those convex areas in different scales. In this study, we simply use “OR” operation to combine the entire convolution outputs at each scale. The reason that allows us to do this is the convex area in larger scale can always include the convex area in smaller scale. Therefore, after we use “OR” operation to combine all scale’s convolution outputs, the convex areas comes from different scales will be merged together.

2.3 Extracting anomalous patches using threshold

The convex areas in different scales acquired in last section are only potential anomalies. To finally conclude a convex area is an anomaly, we need to check the mean of normalized distance for all pixels in this patch. The selection of threshold used for assessing a patch is based on the cumulative distribution function of normalized distance. In this study, the threshold is set to the value that corresponding to 90% of cumulative distribution. A patch will be concluded as an anomaly if the patch mean is greater than threshold.

3 EXPERIMENTAL RESULTS

In this study, two experiments containing different characteristic of anomalies are test.

3.1 Case 1

In this case, the source image is SPOT-5 multi-spectral image. The image acquisition date was on 03/30/2006. The location is in south of Chinese Taipei. Fig. 2 shows the test image for this case. Notice that the anomalies in this dataset are darker than the background. Fig. 3 is the extracted anomalies using proposed scheme.

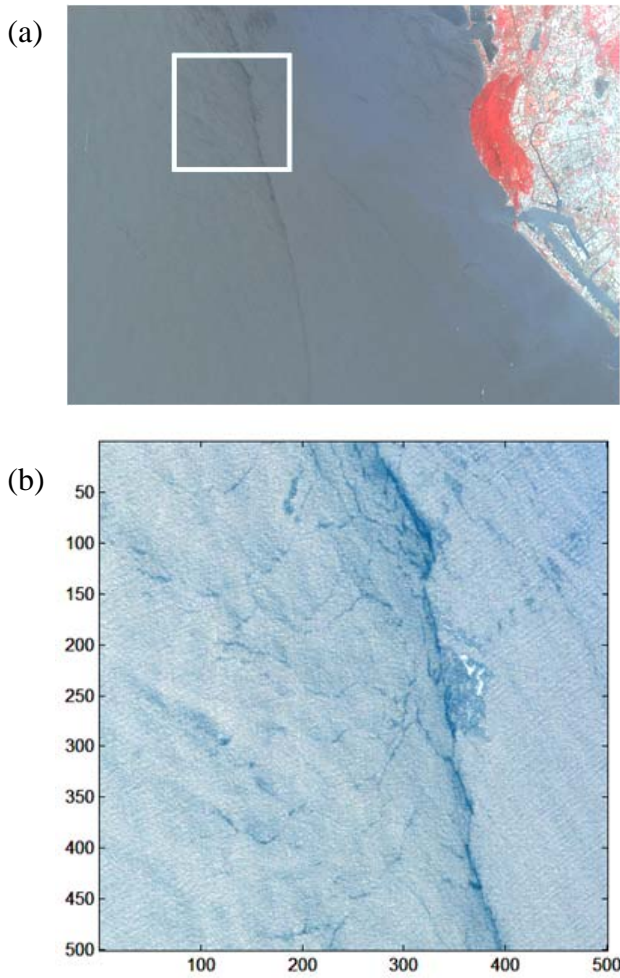


Fig. 2: The test image for case 1, (a) source image and study area for this case, (b) enlarged and enhanced image of study area.

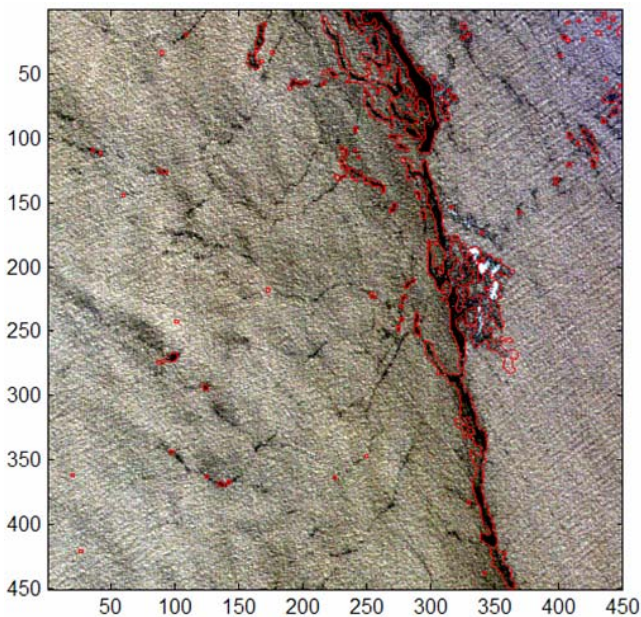


Fig. 3: The extracted anomalies overlay on source image

3.2 Case 2

In this case, the source image is also SPOT-5 multi-spectral image. The image acquisition date was on 07/18/2007. The location is in north of Chinese Taipei. Fig 4 shows the test image for this case. Notice that the anomalies in this dataset are brighter than the background. Fig. 5 is the extracted anomalies using proposed scheme.

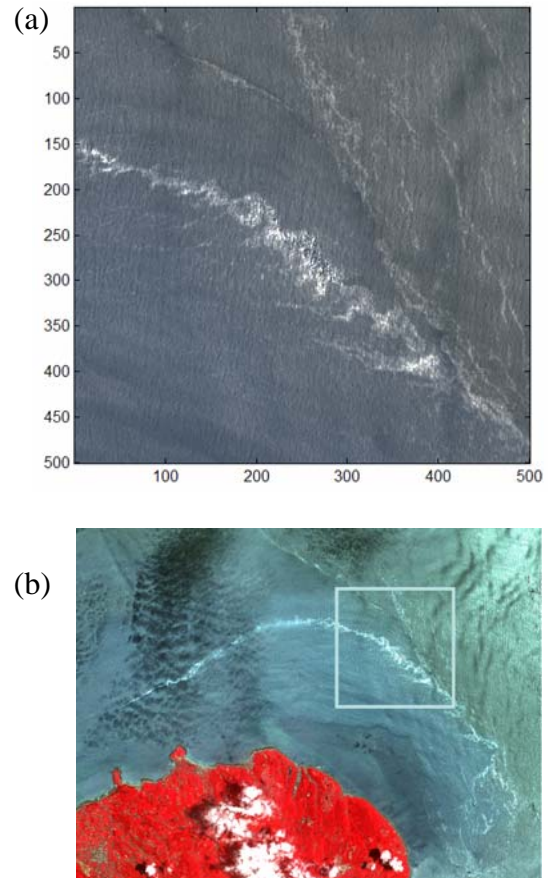


Fig. 4: The test image for case 2, (a) source image and study area for this case, (b) enlarged and enhanced image of study area.

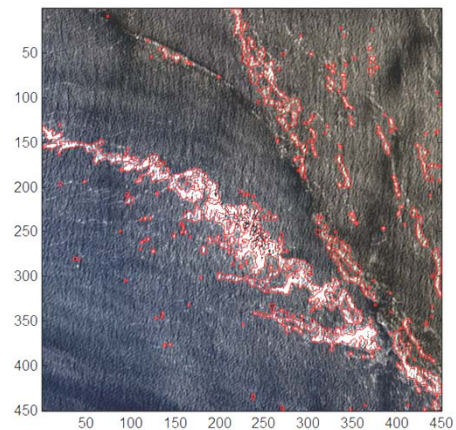


Fig. 5: The extracted anomalies overlay on source image

4. CONCLUSIONS

On ocean surface, the proposed scheme can successfully extract different kinds of anomalies using optical satellite images. Using RXD to retrieve normalized spectral distance enables that various kinds of anomalies can be extracted at the same time. With multi-scale Laplace of Gaussian operator, the noise is effectively reduced and the anomaly in different size can be separated to its corresponding scales for further processing.

The anomalies in larger scale tend to have a smoother boundary because of the stronger smooth effect introduced by large scale Laplace of Gaussian operator. Such problem may be solved by setting up a buffer zone along the boundary and using the anomalies detected in a smaller scale to replace those in this zone. This procedure can be used iteratively until the smallest scale is reached. The only fixed threshold used in proposed scheme is the normalized distance value at 90% of the cumulative distribution. A more adaptive way for estimating this threshold should be carried out to relax this limitation in future researches.

REFERENCES

- Brown CE, Fingas MF (2001) New space-borne sensors for oil spill response, Proceedings of International Oil Spill Conference 2001, Tampa, Florida: 911-916
- Keeler RN, Bondur VG, Gibson CH (2005) Optical satellite imagery detection of internal wave effects from a submerged turbulent outfall in the stratified ocean, Geophysical Research Letters, 32: L12610
- Reed IS, Yu X (1990) Adaptive multiple-band CFAR detection of an optical pattern with unknown spectral distribution, IEEE Transactions on Acoustic, Speech and Signal Processing, 38(10): 1760-1770
- Pratt WK (1991) Digital image processing, Wiley, New York
- Chang CI, Heinz D (2000) Constrained subpixel detection for remotely sensed images, IEEE Transactions on Geoscience and Remote Sensing, 38(3): 1144-1159

Simulation of Spilled Oil in Seribu Islands Waters

Safwan Hadi^{1,2}, Totok Suprijo¹, Haris Sunendar²
 1 Resarch Group of Oceanography, ITB
 2 Center for Marine and Coastal Development, ITB



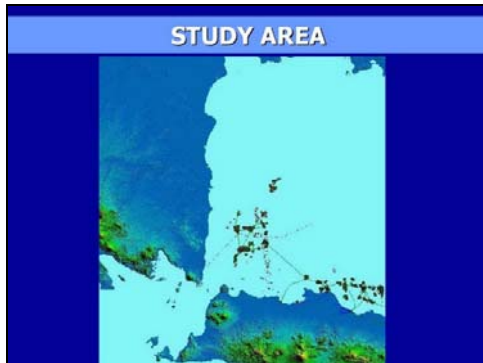
GOVERNING EQUATIONS

Continuity Equation:

$$\frac{\partial \zeta}{\partial t} + \frac{\partial U}{\partial x} + \frac{\partial V}{\partial y} = 0$$

Momentum Equation:

$$\frac{\partial U}{\partial t} + U \frac{\partial U}{\partial x} + V \frac{\partial U}{\partial y} + gH \frac{\partial \zeta}{\partial x} + fU \frac{\sqrt{U^2 + V^2}}{H} + A_{ed} \Delta_t^2 U = \lambda W_x \sqrt{W_x^2 + W_y^2}$$

$$\frac{\partial V}{\partial t} + U \frac{\partial V}{\partial x} + V \frac{\partial V}{\partial y} + gH \frac{\partial \zeta}{\partial y} + fV \frac{\sqrt{U^2 + V^2}}{H} + A_{ed} \Delta_t^2 V = \lambda W_y \sqrt{W_x^2 + W_y^2}$$


TRAJECTORY EQUATIONS

Trajectory Equation Caused by Wind and Current

$$XPW(m, n)^{t+\Delta t} = XPW(m, n)^t + \Delta t (U_x^{t+\Delta t} + 0.03 U_w + (\mu - 0.5) P_u)$$

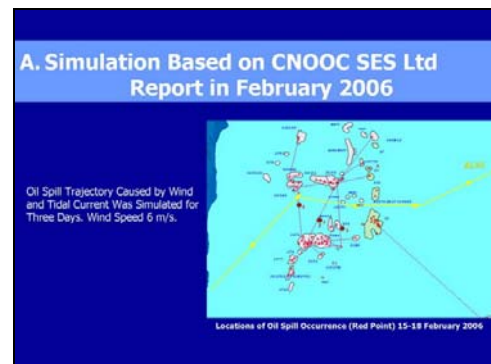
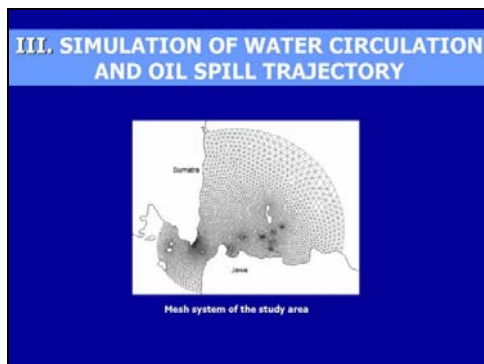
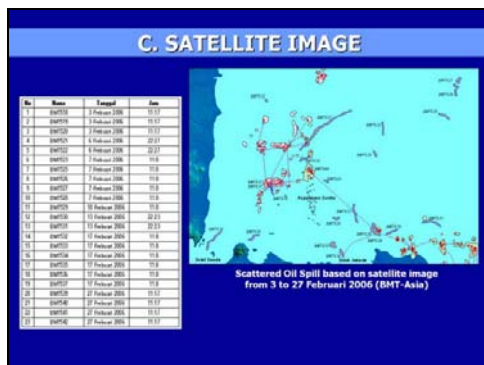
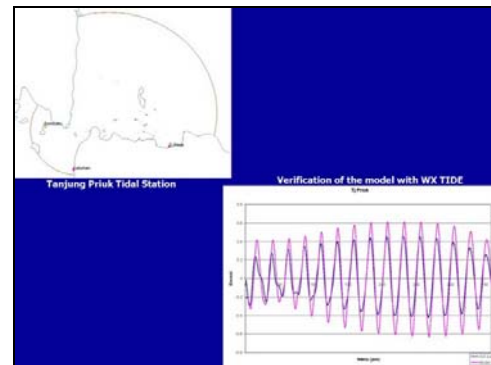
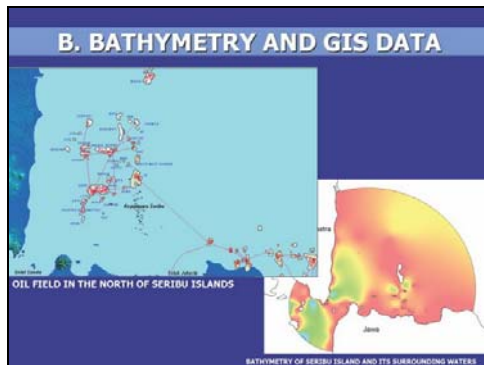
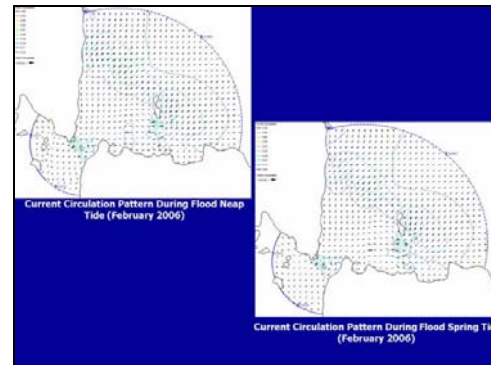
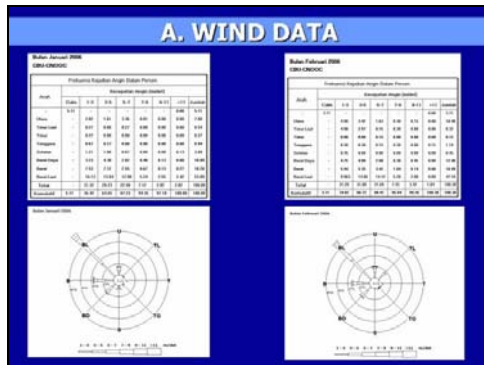
$$YPW(m, n)^{t+\Delta t} = YPW(m, n)^t + \Delta t (V_y^{t+\Delta t} + 0.03 V_w + (\mu - 0.5) P_v)$$

I. OBJECTIVE OF THE STUDY

1. To Develop Oil Spill Model For Seribu Islands Waters – North Of Jakarta.
2. To Use The Model to Predict The Movement of Spilled Oil from Oil Field in the North Of Seribu Islands.

II. DATA USED FOR THE SIMULATION


- A. WIND DATA
- B. BATHYMETRY AND GIS DATA
- C. SATELLITE IMAGE



B. Simulation Based on Interpretation of Satellite Image

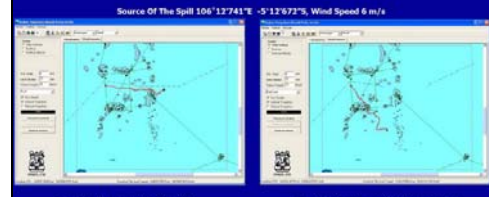
Analysis of Oil Spill Occurrence Based on RADARSAT Image – 1 Wide Beam 3 by BMT – Asia Pacific PTE Ltd for CNOOC SES Ltd, February 2006.

There Were 23 Oil Spill Occurrences During February 2006.



Scattered Oil Spill based on satellite image from 3 to 27 February 2006 (BMT-Asia)

Source Of The Spill 106°12'741"E -5°12'672"S, Wind Speed 6 m/s



Simulation for 72 hours, Wind from West, Travelling Distance 46327.06 meter

Simulation for 72 hours, Wind from NorthWest, Travelling Distance 44859.21 meter

C. Trace Back Simulation Based on Spilled Oil Found in Bira Island (Seasonal Variation)

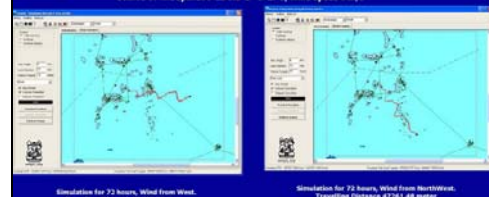
Trace Back Simulation From Bira Island With Wind Data From CBU for 240 Hours From February 19 2006

D. Simulation Based on Observed Daily Wind Data at CBU Station.

Based on the Fact Found in The Field There Are Two Patterns of Oil Spill Occured in Seribu Islands :

- East Monsoon → Spilled Oil Found Around Pramuka Island
- West Monsoon → Spilled Oil Found Around Bira Island

Source Of The Spill 106°13'5.5"E -5°17'S, Wind Speed 6 m/s



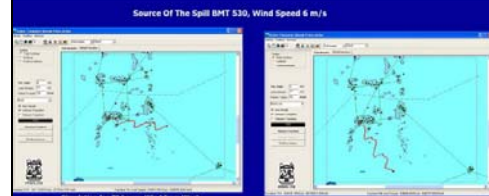
Simulation for 72 hours, Wind from West, Travelling Distance 45297.08 meter

Simulation for 72 hours, Wind from NorthWest, Travelling Distance 47251.48 meter

RESULTS OF OIL SPILL SIMULATION

B. Simulation Based on Interpretation of Satellite Image

Source Of The Spill BMT 530, Wind Speed 6 m/s




Simulation for 72 hours, Wind from West, Travelling Distance 46441.89 meter

Simulation for 72 hours, Wind from NorthWest, Travelling Distance 46752.02 meter

A. Simulation Based on CNOOC SES Ltd Report in February 2006

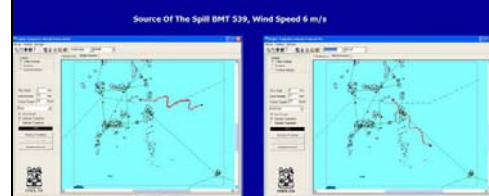
Source Of The Spill 106°13'285"E -5°12'541"S, Wind Speed 6 m/s



Simulation for 72 hours, Wind from West, Travelling Distance 47894.74 meter

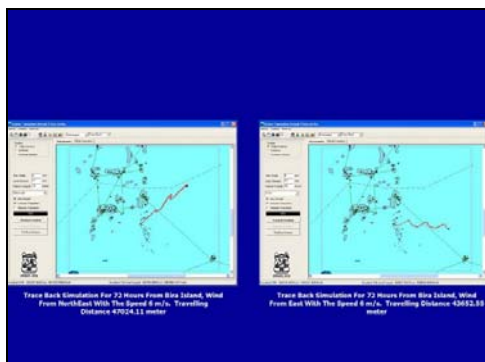
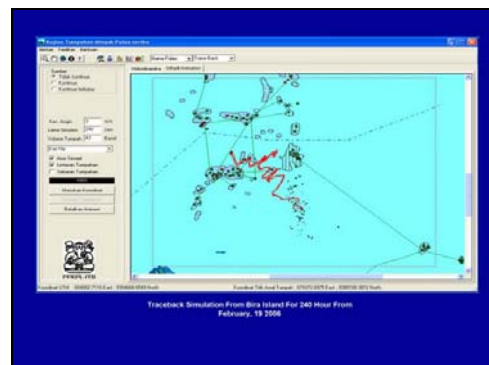
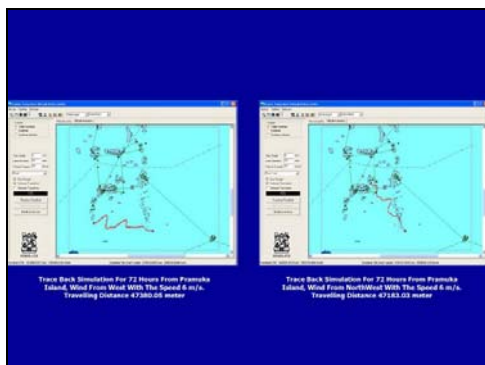
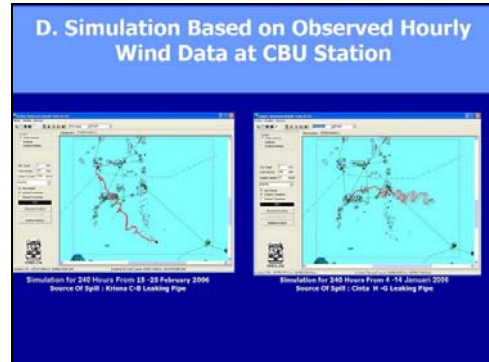
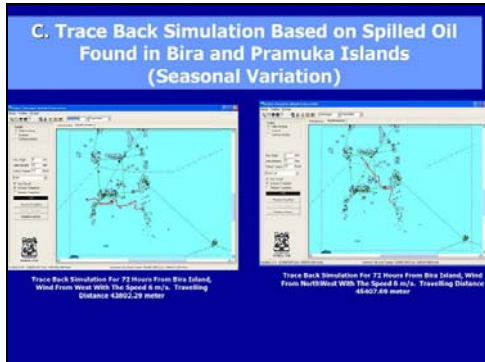
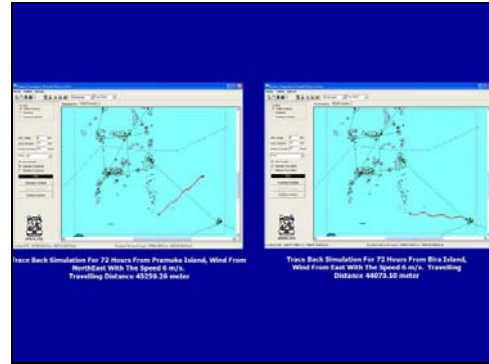
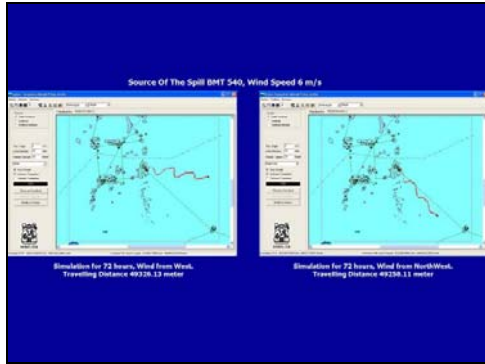
Simulation for 72 hours, Wind from NorthWest, Travelling Distance 46402.33 meter

Source Of The Spill BMT 539, Wind Speed 6 m/s



Simulation for 72 hours, Wind from West, Travelling Distance 46630.72 meter

Simulation for 72 hours, Wind from NorthWest, Travelling Distance 46136.21 meter



IV. CONCLUSION

1. Oil Spill Model Develop in The Study Show Good Capability of Simulating Oil Spill Trajectory in Seribu Islands Water.
2. Oil Platform Situated in the North of Seribu Islands are Potential threat for Oil Pollution in Seribu Islands.
3. Local Government of Seribu Islands Should Develop Mitigation Plan to Reduce the Risk of Oil Pollution in Seribu Islands in The Future.